AIAA JOURNAL
Vol. 42, No. 6, June 2004

Flow Around a Rotatable Circular Cylinder–Plate Body at Subcritical Reynolds Numbers

Yahya Erkan Akansu,* Mustafa Sarioglu,† and Tahir Yavuz‡
Karadeniz Technical University, 61080 Trabzon, Turkey

The behavior of a stationary circular cylinder with an attached plate, under conditions where the entire cylinder–plate body rotates about the cylinder axis, has been investigated experimentally for Reynolds numbers between 8×10^3 and 6×10^4. To see the effect of the plate inclination on the pressure distributions and vortex shedding, the cylinder–plate body was rotated from 0 to 180 deg, unlike freely rotatable cases in previous studies. The plate was located at the center plane of the cylinder, upstream of the cylinder, at the beginning. The diameter of the cylinder and the width of the plate were both chosen to be 35 mm. Measurements of shedding frequency and pressures on the surface of the cylinder were obtained. The results indicate that the shedding frequency was nearly constant in the range of 50–120 deg and, by further increasing the angle from 120 to 160 deg, it strikingly increases and then again decreases at angles larger than 160 deg. The plate also causes important changes in pressures on the surface of the cylinder with increasing inclination angle. For different plate angles, five different types of pressure distributions have been observed. Characteristics of the vortex formation region and location of flow attachments, reattachments, and separations were observed by means of the flow visualizations. The drag coefficient of the cylinder has a maximum value at approximately $\theta = 75$ deg, whereas it has a minimum value at $\theta = 15$ deg. The lift coefficient has two maximums, at $\theta = 15$ and 165 deg, depending on the plate position. The values of C_L at about $\theta = 45$ and 160 deg are zero as in the case of the cylinder without a plate.

Nomenclature

C_D = drag coefficient
$\frac{1}{2}\int_0^{2\pi} C_p \cdot \cos\alpha \, d\alpha$
C_L = lift coefficient
$-\frac{1}{2}\int_0^{2\pi} C_p \cdot \sin\alpha \, d\alpha$
C_p = pressure coefficient, $(P - P_{st})/\frac{1}{2}\rho U^2$
D = diameter of circular cylinder
D' = projected cross-stream dimension of the cylinder–plate body
f = vortex-shedding frequency
L = width of the plate
P = surface pressure
P_{st} = static pressure in the test section
Re = Reynolds number based on D, UD/ν
Sr = Strouhal number, fD/U
Sr' = Strouhal number, fD'/U
U = freestream velocity
x, y = streamwise and lateral coordinates
α = circumferential angle measured from the stagnation point of the cylinder
θ = plate angle
ν = kinematic viscosity of fluid
ρ = density of air

Received 31 July 2003; revision received 12 January 2004; accepted for publication 5 March 2004.

*Research Assistant, Department of Mechanical Engineering; akansu@ktu.edu.tr.
†Research Assistant, Department of Mechanical Engineering.
‡Professor, Department of Mechanical Engineering.

I. Introduction

EXPERIMENTAL studies have shown that the flow of the wake of a circular cylinder can be strikingly changed by a splitter plate. It was concluded that a splitter plate either attached or placed in the wake of bluff bodies can reduce the drag and the strength of the vortex shedding. Detailed information about splitter plates are available in a series of papers.[1–16]

The behavior of a circular cylinder with attached splitter plate under conditions where the entire cylinder/splitter plate body was free to rotate about the cylinder axis has been studied experimentally in Ref. 1. It has been observed that a cylinder/splitter plate model rotates to an equilibrium position off the centerline at both subcritical and supercritical Reynolds numbers. For any given L/D, the equilibrium angle decreases suddenly in the transitional Reynolds number regime, where the boundary-layer separation on the cylinder changes from laminar to turbulent. At supercritical Reynolds numbers, angle θ (starting from the back base point of the cylinder) rises slowly and then levels off at very high Reynolds numbers to a value significantly smaller than that at subcritical Reynolds numbers. It was found that the transition Reynolds number range for the cylinder with very short plate lengths ($L/D \approx 1/8$) was around 2.5×10^5–3.5×10^5. For longer splitter plate lengths, the critical Reynolds number was lower; the transition Reynolds number range was around 1.5×10^5–2.0×10^5.

In Ref. 2, flow visualization, hot-wire, and base pressure measurements were conducted for an investigation of the near wake of a circular cylinder at subcritical Reynolds numbers between 2.7×10^3 and 4.6×10^4. A base-mounted splitter plate allowed for the modification of the formation region characteristics without disrupting the normal von Kármán shedding. The results provide an explanation for the nonlinearity in the relationship between shedding frequency and splitter plate length.

The flow around a circular cylinder with a few interference elements shifted along the wake was investigated in Ref. 3. It was concluded that the vortex shedding can be suppressed critically even when the splitter plates are asymmetrically arranged behind the cylinder.

An experimental investigation was carried out to study the effect of a splitter plate on the two-dimensional wake of a bluff body with fixed separation points.[4] This experimental study has shown that the characteristics of the wake downstream of a bluff body with

fixed separation points can be considerably altered by placing a splitter plate on the wake centerline downstream of the bluff body. The effect of splitter plates on the wake flow characteristics of a rectangular cylinder with a splitter plate shows a relatively small change in Reynolds number.

In Ref. 5, vortex shedding from bluff bodies with splitter plates was experimentally investigated. It was shown that vortex shedding from bluff bodies with extended splitter plates is characterized by the impinging shear layer instability, where the Strouhal number in terms of splitter plate length increases stepwise with increasing splitter plate length.

The aerodynamic properties and the mechanisms of the aerodynamic behaviors on two-dimensional tandem bluff bodies were investigated by measurements of unsteady pressure distributions around the cylinders and by using the flow visualization technique.[6] Both the accelerated "gap flow" and the accelerated "outside flow" around the downstream cylinder played important roles in the violent crosswind oscillation of two tandem circular cylinders with a spacing ratio of $L^*/D = 3$. The violent crosswind oscillation of the single circular cylinders with a splitter plate had a similar mechanism to that of conventional galloping of a two-dimensional rectangular cylinder from the standpoint of being caused by the existence of an inner circulatory flow.

In Ref. 9, measurements of instantaneous pressure fluctuations on a trapezoidal cross-sectional cylinder indicate that the low-frequency variations embedded in the vortex-shedding process can be successfully suppressed by insertion of a splitter plate whose length is twice the maximum width of the trapezoidal cylinder.

The angular motion of a freely rotatable cylinder with splitter plate has been studied numerically in Ref. 11. It is found that, for subcritical Reynolds numbers, the splitter plate aligns itself in the flow direction. On increasing the Reynolds number, a symmetry-breaking bifurcation appears and the splitter plate migrates to a stable off-axis position.

The flow in the wake of a freely rotatable cylinder with splitter plate has been investigated experimentally in Ref. 12. Smoke-wire flow visualizations were compared for three cases: 1) a plane cylinder, 2) a cylinder with a splitter plate 1 diam long and fixed parallel to the freestream direction, and 3) the same cylinder/splitter plate body but freely rotating. In case 3), it rotated to a stable angle of approximately 22 deg for a Reynolds number of 7.5×10^3. And also it is revealed that the wake of the freely rotatable cylinder/splitter plate body is not grossly different from that of the plain cylinder. When fixed at 0 deg, however, the splitter plate significantly alters the wake. Specifically, the fixed splitter plate forces a delay in the formation of the von Kármán vortex street.

The effects of drag reduction produced by ribbons attached to cylindrical pipes have been investigated experimentally in Ref. 16. This experiment demonstrated that attached ribbons can be used to reduce the drag force on vertical pipes for various directions of incoming flow.

Some of the experiments just outlined considered the flow, drag, and vortex characteristics about a freely rotatable cylinder/plate body, so that the system is an equilibrium stage where the splitter plate is freely positioned at the equilibrium angle. In the present study, unlike some previous studies mentioned earlier, the cylinder and plate were not freely rotatable, and the plate was able to be located at any desired inclination angle to the flow. Hence, the major purpose of this study is to investigate the effect of the plate with various inclination angles on the flowfield, pressure, and vortex-shedding characteristics around the cylinder.

II. Experimental Apparatus and Procedure

The experiments were conducted in the test section of a low-speed, open-type wind tunnel. The test section measures 289 mm wide, 457 mm high, and 1830 mm long. The two side Plexiglas® walls of the test section are tapered with a divergence angle of 0.3 deg on each side to give constant static pressure and to compensate for boundary-layer growth along the tunnel axis. Details involving the test section can be found in the paper by Sarioglu and Yavuz.[17] At the maximum tunnel speed of about 36 m/s, the freestream turbulence intensity was about 0.5%. The Reynolds number was in the range of 8×10^3–6×10^4 in the study, corresponding to a freestream velocity of about 3.5–25 m/s, respectively. The tunnel and test section are shown in Fig. 1. The circular cylinder was centered on the midheight of the test section, and spanned width of the test section. The configuration of the circular cylinder with an attached plate is shown in Fig. 2. The diameter of the circular cylinder tested, D, was 35 mm and the width of the plate, which was made of stainless steel, attached to the cylinder was also 35 mm, that is, $L/D = 1.0$, and its thickness was 1 mm. The circular cylinder has one pressure tap of 0.7 mm in diameter on its surface. The angles α and θ defined in Fig. 2 are the circumferential angle measured from the stagnation point on the cylinder and the inclination angle of the plate, respectively. The cylinder–plate body was positioned at an angle of incidence to the freestream flow direction and turned in the range of $0 \text{ deg} \leq \theta \leq 180$ deg with the accuracy of ± 0.5 deg. The blockage ratio was about 7.7% at $\theta = 0$ deg.

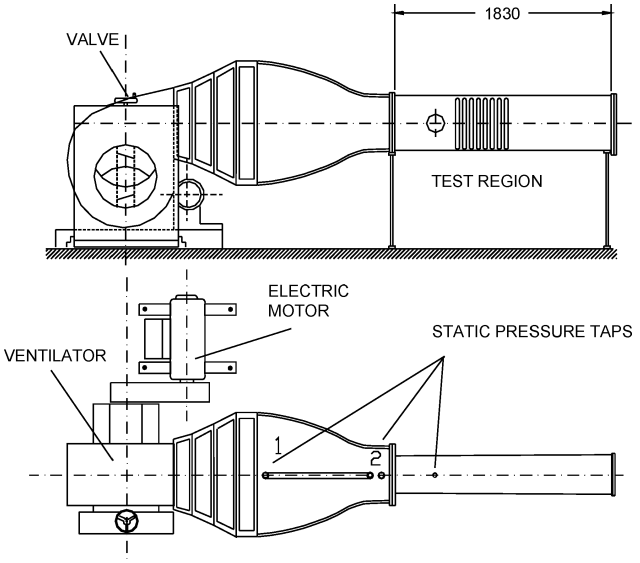

Fig. 1 Low-speed, open-type wind tunnel and test section.

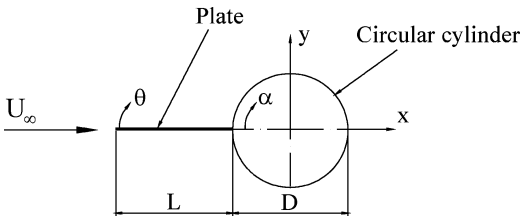

Fig. 2 Flow configuration and symbol definition.

Vortex shedding from the cylinder–plate body was detected by using a TSI intelligent flow analyser Model 100 constant-temperature anemometer with a hot-film probe. The Strouhal numbers for the vortex shedding from the model were determined from the frequency analysis of the velocity fluctuations. The probe was located in the center plane of the test section at approximately $4D$ downstream of the cylinder and was mounted on a traversing mechanism that could move it in the transverse direction in the range $-5 < y/D < 5$. Pressure measurements were made with a pressure transmitter in conjunction with a TSI Model 157 signal conditioner. The transmitter was connected to the pressure taps in reference to the freestream wall pressure.

Velocity and pressure measurements were carried out by using a computer-controlled data acquisition system. For velocity measurements at each measurement point, 4096 data points were acquired at a sampling rate of 1 kHz using a low-pass filter setting of 300 Hz. The pressure signals were acquired at a rate of 200 samples/s and were low-pass filtered at 100 Hz. Each of the mean pressures was obtained by means of integrating the time history of 8192 data points for over 40 s. TSI Thermal-Pro software was used to acquire

signals with a 12-bit A/D converter and obtain the statistical results of these signals. The experimental uncertainties in the measurement of velocity and pressure were determined to be less than ±3 and ±4%, respectively. Blockage correction was not made because of flow asymmetry.

III. Experimental Results and Discussion

A. Velocity Measurements

Velocity profiles in the wakes of the circular cylinder with the plate were measured at only one Reynolds number, 2.0×10^4. Velocity profiles obtained at the station $x/D = 4.0$ in the wake of the cylinder with and without the plate at various inclination angles are shown in Fig. 3.

In the velocity distributions, the location of the minimum velocity is on the center of the wake for $\theta = 0$ deg; then it moves in the downstream direction as θ increases from 0 to 15 deg. With increasing angle of the plate the wake moves farther above the centerline up to $\theta = 135$ deg, and then it again moves on the centerline at $\theta = 150$ deg. This can be explained as follows. At $\theta \leq 10$ deg, attached shear layers on the lower surface of the plate–cylinder are inclined toward the lower side of the cylinder depending on the plate angle. Thus, the lower boundary of the wake moves downstream while the upper one does not change. With $\theta = 15$ deg, the separation of the flow from the leading edge of the plate does not reattach on the cylinder and the upper boundary of the wake begins to move in the upward direction. With further increase in plate angle, the cylinder–plate body behaves as a bluff body and the increased projected area increases the width of the wake. These points are also seen in the flow visualization test given in Fig. 4.

B. Mean Pressure Distributions

The phenomenon of vortex shedding from a circular cylinder–plate body depends largely on angle of incidence to the flow. The unsteady flow in the vortex formation process may have reverse flow and reattachments may occur intermittently. However, the attachments and separations on some points of the cylinder–plate body due to approaching flow are inevitable. Locations of these points can be determined from mean pressure distributions and also from flow visualization photographs.

The mean pressure distributions on the surface of the cylinder with and without a plate were obtained for the Reynolds number of 2.0×10^4 for the angles of the plate, θ, in the range 0–180 deg. Results are presented in Fig. 5. As shown in this figure, there are five types of pressure profiles. The first group is obtained at $\theta = 0$ and 180 deg and for no plate. The pressure distributions obtained for these three cases have the same characteristics. But, in the case of $\theta = 180$ deg, for which the plate is in the wake of the cylinder, pressure on the base of the cylinder has a higher value compared with the values obtained for the other two cases. In this case, vortices behind the cylinder are formed farther downstream in the wake of the cylinder. As a matter of fact, Roshko[18] found that a splitter plate of length D in contact with the cylinder did not inhibit the vortex formation, but it caused approximately a 20% reduction in shedding frequency and approximately a 35% increase in the base pressure compared with the values for the cylinder alone.

The second group is obtained at $\theta = 5$, 10, and 15 deg. At these angles, the projected area of the plate–cylinder body does not change. At the angles of $\theta = 5$ and 10 deg, the stagnation point moves to the lower side of the cylinder, occurring at $\alpha = 340$ and 350 deg at $\theta = 5$ and 10 deg, respectively, whereas it occurs at $\alpha = 0$ deg for $\theta = 15$ deg. The maximum at $\alpha = 40$ deg and the minimum at $\alpha = 80$ deg in the pressure distribution for $\theta = 5$ deg indicate attachment and separation from the surface of the cylinder, respectively. At $\theta = 10$ deg the weak attachment occurs at $\alpha = 60$ deg and the separation point moves at $\alpha = 90$ deg. Finally, at $\theta = 15$ deg, there is no attachment on the upper surface.

The third group is those measured at 30 deg $\leq \theta \leq 90$ deg. Here, with the angle of $\theta = 30$ deg, the projected area begins to increase and it reaches a maximum at $\theta = 90$ deg and the plate behaves gradually as a bluff body. The pressure increases and the stagnation point moves to the upper side of the cylinder. After the pressure of this stagnation point, the pressures becomes constant until the angle α corresponds to the angle of the plate, θ. And after this angle, there is a sudden drop in pressure and negative pressures occur.

The fourth group is obtained at 105 deg $\leq \theta \leq 150$ deg. At these inclination angles, flow separated on the upper surface of the cylinder at about $\alpha = 60$ deg reattaches on the surface of the plate and then flow again reseparates at the trailing edge. Hence, there are two separation points, first on the upper surface of the cylinder and second at the trailing edge of the plate. In addition to the two separation points, there is also another separation point on the lower surface of the cylinder. With increasing inclination angle, the reattachment point of the shear layer on the plate moves toward the end of the plate. At these angles, the shear layer flow between the upper surface of the cylinder and the reattachment point on the plate can be seen in the flow visualization test given in Fig. 4 at the corresponding angles. Consequently, there are two pressure drops in the pressure distribution.

The fifth group is obtained at $\theta = 165$ deg. At this inclination angle, separated flow at the upper surface of the cylinder does not reattach on the plate. Because of this, there is an increase rather

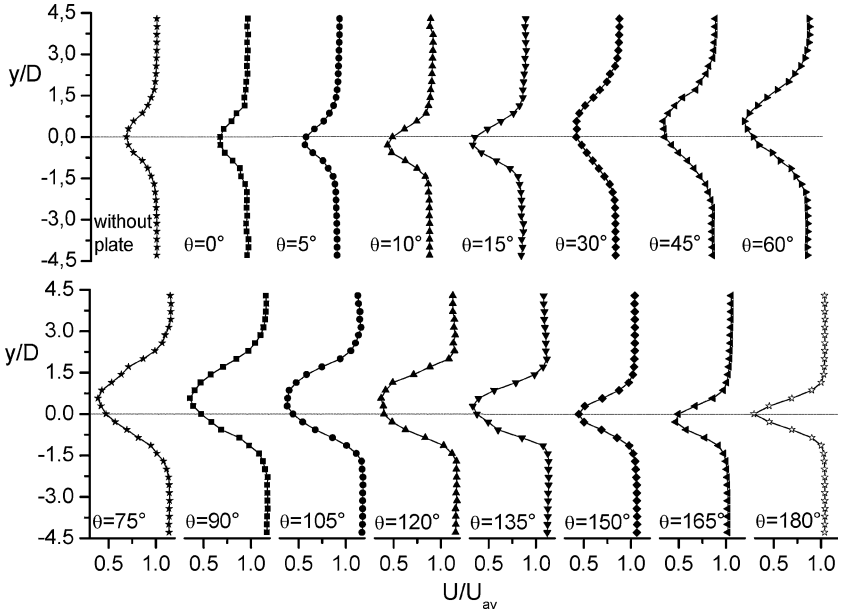

Fig. 3 Dimensionless velocity distributions at $x/D = 4.0$ in the wake of the circular cylinder.

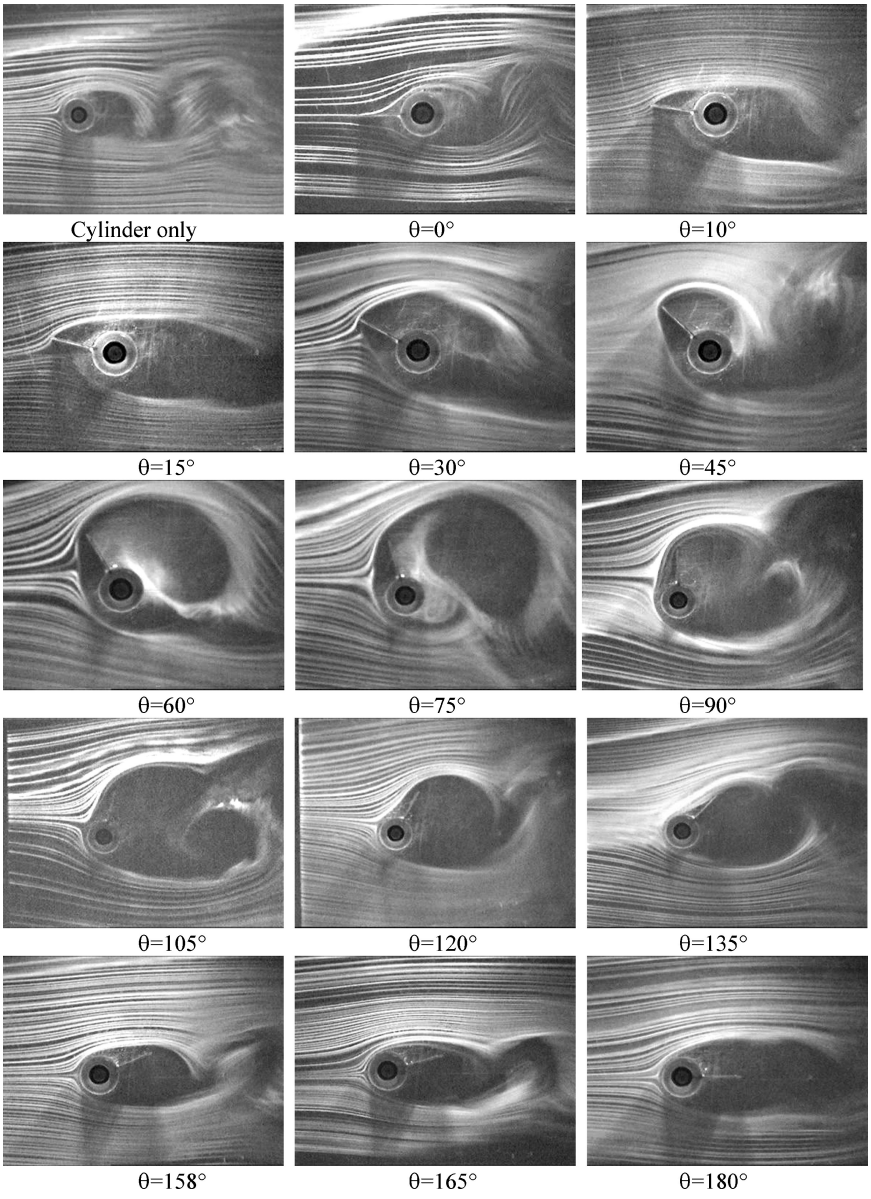

Fig. 4 Smoke-wire visualization of the flow around the cylinder–plate body for $Re = 8 \times 10^3$.

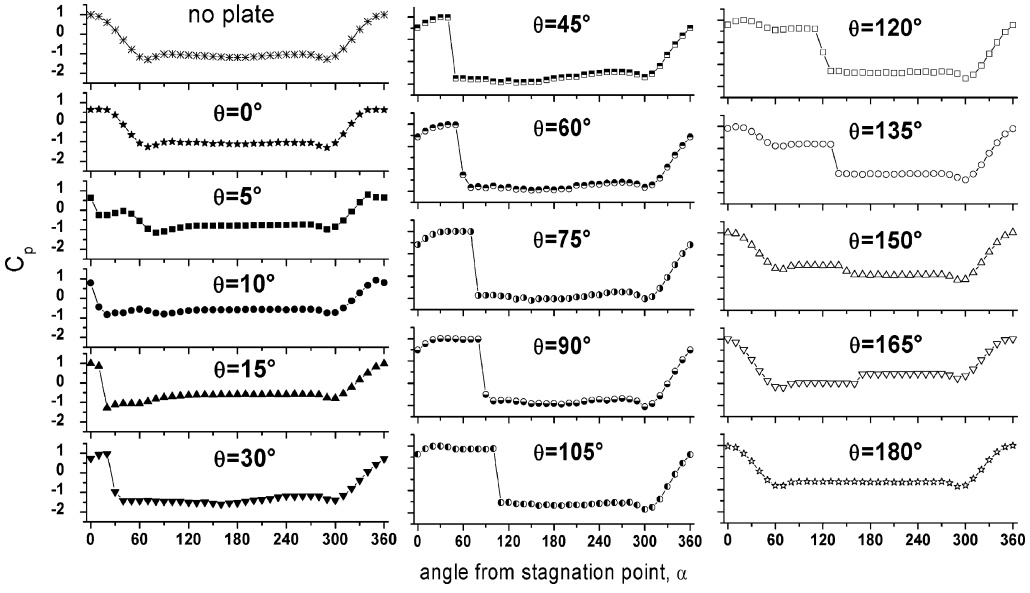

Fig. 5 Pressure distributions around circular cylinder.

than decrease in the pressure at that location ($\alpha = 165$ deg) on the cylinder surface. In Refs. 1 and 12, in the case of the freely rotating splitter plate, it is mentioned that the equilibrium angle is about 158 deg for the plate of D length. At this angle, the splitter plate divided the flow into two parts and the bottom separation bubble increased in size while the upper one decreased in size. This causes an imbalance in the pressure force on either side of the plate. This imbalance in force causes the system to move toward the equilibrium angle. Therefore, at $\theta = 165$ deg, which is nearest to the equilibrium angle, the pressure increases at that location on the surface of the cylinder.

C. Flow Visualization

To see the flowfield about the cylinder–plate arrangement, the flow visualization experiments were conducted by using the smoke-wire method in the wind tunnel with the same model for $Re = 8 \times 10^3$ (Fig. 4). As shown in this figure, for $\theta = 0$ deg, the wake of the cylinder–plate body is not completely different from that of the cylinder alone. In these two cases, the separation points on both the upper and lower sides of the cylinder correspond to nearly the same angles. At small values of θ, 0–10 deg, the plate divides the flow into two parts and flow on the upper side separates from the end of the plate, then reattaches on the cylinder continuously. As seen from the photograph for $\theta = 15$ deg, reattachments of the separated shear layer no longer occur. But with the bigger values of θ, reverse flow in the vortex formation region may reattach on the back side of the cylinder intermittently. The width of the wake reaches its maximum value at $\theta = 90$ deg. As the angle increases, the location of the reattachment on the plate gradually moves to the tip of the plate. This phenomenon is seen clearly at $\theta = 135$ deg. Considering Figs. 4 and 5 together, flow visualizations confirm the pressure distributions presented in Fig. 5. And, considering Figs. 3 and 4 together, it is distinctly noticed why the location of the minimum velocity moves to the upper or lower side of the centerline. At near equilibrium angle, $\theta = 158$ deg, separations occurred on both upper and lower surfaces of the cylinder but there was no reattachment on the plate. In the case of the splitter plate, that is, at 180 deg, the flow is divided into two parts. Compared to with the cylinder alone, the plate at 180 deg considerably changes the wake and it causes variation of the distance required for vortex formation behind the body.

D. Spectral Measurements and Strouhal Numbers

Spectra measured at different plate angles between 0 and 180 deg are presented in Fig. 6. They were obtained at the position $x/D = 4$, $y/D = 2$ in the wake of the circular cylinder to preclude interference in the velocity signal from vortices of opposite sign. As shown in this figure, with θ increasing from 0 deg, there is a slight increase in vortex-shedding frequency up to $\theta = 6$ deg, whereas there is considerable decrease at 8–40 deg. The vortex-shedding frequency remains almost constant at 50–120 deg. With further increase in θ, the frequency increases considerably at 120–160 deg and then decreases again.

Strouhal numbers Sr and Sr' calculated using vortex-shedding frequencies obtained from spectral distributions, are shown in Fig. 7. The Strouhal number has two maximums at $\theta = 6$ and 162 deg in the range 0 deg $\leq \theta \leq$ 180 deg. When examining Strouhal numbers together with pressure distributions, at $\theta = 5$ deg, the increase in Strouhal number at smaller plate angles is associated with the separation of the shear layers from the upper side of the cylinder and the stagnation point moves from $\alpha = 0$ deg to $\alpha = 340$ deg. After the maximum value of Strouhal number at $\theta = 6$ deg, the effect of the separation of the shear layer gradually decreases. Then, after $\theta = 10$ deg, the separation occurs on the leading edge of the plate and there is no separation from the upper surface of the cylinder. This corresponds to a decrease in Strouhal number. For some values of θ, where the projected height of the cylinder–plate body increases, Strouhal number has small values depending on the decrease in frequency. Strouhal number Sr', has higher values than those of Sr. After $\theta = 120$ deg, with considerable decrease in the projected height, Strouhal number increases until $\theta = 162$ deg, and then decreases again to reach the small value at $\theta = 180$ deg. This value of Strouhal number at $\theta = 180$ deg is 0.151. It is approximately 22% smaller than that of the circular cylinder without the plate.

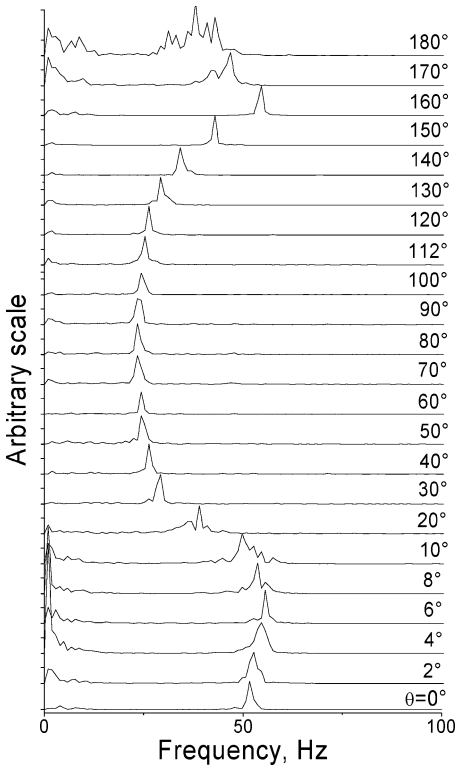

Fig. 6 Spectrums measured at $x/D = 4$, $y/D = 2$ in the wake of the circular cylinder.

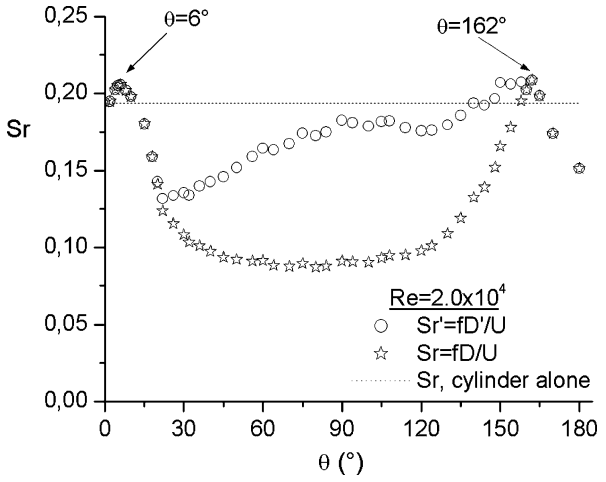

Fig. 7 Strouhal number vs incidence angle θ.

Figure 8 shows Strouhal number as a function of Reynolds number for various considered plate angles. Data were acquired at about 20 different wind-tunnel speeds for each plate angle θ, giving a Reynolds number range of about 8×10^3–6×10^4. For a given plate angle, especially at $\theta \geq 10$ deg, Strouhal number was found to be largely independent of Reynolds number. In the cases of $\theta < 10$ deg, there is a little increase in Strouhal number especially in the range of $Re = 5.0 \times 10^4$–6.0×10^4. In general, as seen in this figure, Strouhal number has not changed with Reynolds number considerably. Also, it can be said that, in this Reynolds number range, the flow type has changed only with the plate angle. As a matter of fact, Apelt and West[19] explained that over the Reynolds number range 10^4–5.0×10^4, pressure distributions and Strouhal numbers were found to be independent of the Reynolds number. Therefore, in the present study the flow visualizations conducted in $Re = 8 \times 10^3$

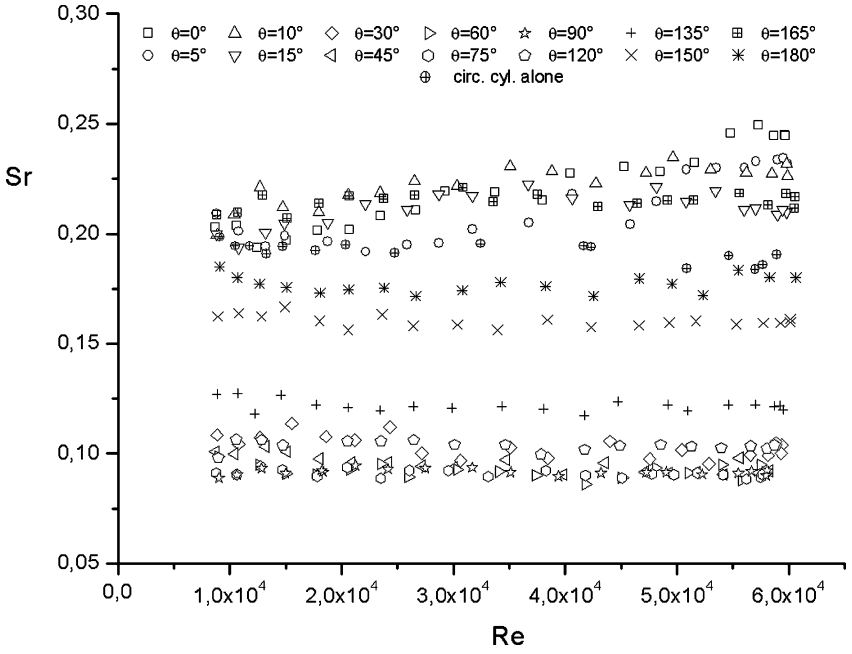

Fig. 8 Distribution of the Strouhal number of the cylinder–plate body for different Reynolds number.

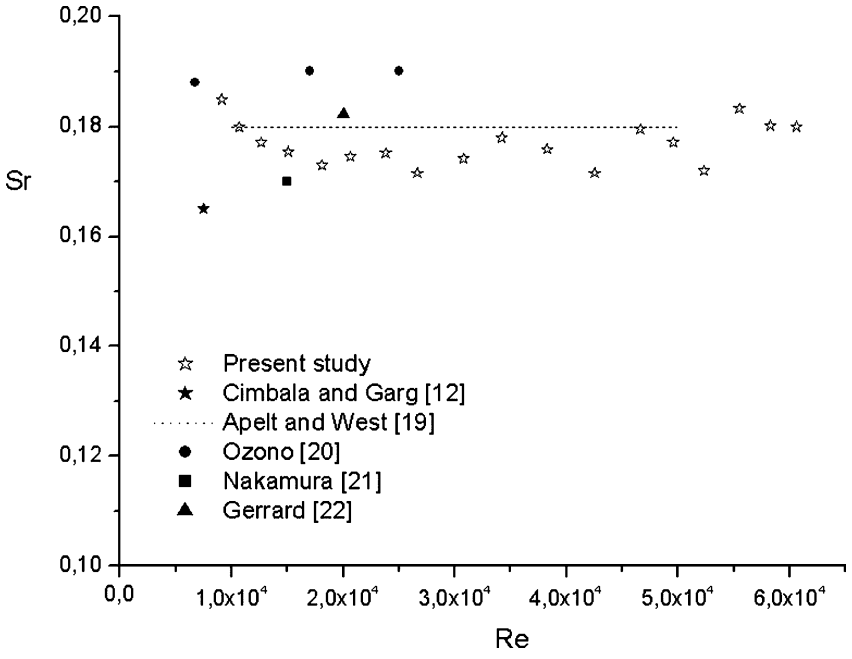

Fig. 9 Variation of Strouhal number vs Reynolds number for comparison with previous studies for $\theta = 180$ deg.

(Fig. 4) can be adopted to simulate the corresponding flow behavior measured in the wind tunnel. Figure 9 shows the comparison between some previous studies and the present result for $L/D = 1.0$ and $\theta = 180$ deg. In these previous studies related to splitter plates, the variations of Strouhal number with L/D were largely investigated. As shown in the figure, the present result remains among the results of Cimbala and Garg,[12] Apelt and West,[19] Ozono,[20] Nakamura,[21] and Gerrard,[22] for only $L/D = 1.0$ and $\theta = 180$ deg.

E. Drag and Lift Coefficients

The drag and lift coefficients of the circular cylinder–plate body are obtained by the integration of the mean pressure distributions on the cylinder and are shown in Figs. 10 and 11. Hence, results include the effect of the plate. The contributions to drag and lift coefficients due to the plate are not considered.

As shown in Fig. 10, depending on the pressure distributions given in Fig. 3, the drag coefficient decreases with increasing plate angle and reaches a minimum value at about $\theta = 15$ deg, because the pressure at $\alpha > \theta$ on the upper front surface of the cylinder is lower than that of the cylinder alone. On the other hand, the pressure increases with θ and reaches a maximum value at about $\theta = 75$ deg because of the increase in pressure at the region of the circumferential angle α smaller than the plate angle (θ) on the front face of the cylinder. After $\theta = 105$ deg, because of the separation that occurred at about $\alpha = 60$ deg, a decrease in pressure causes the drag coefficient to decrease again. At $\theta = 150$–180 deg, the fact that pressure on the back of the cylinder are higher according to the cylinder alone also causes the drag coefficient to be smaller according to the cylinder alone. As noticed from the figure, for plate angles $\theta < 30$ and $\theta > 135$ deg, the drag coefficients are always less; for plate angles 30 deg $< \theta <$ 135 deg,

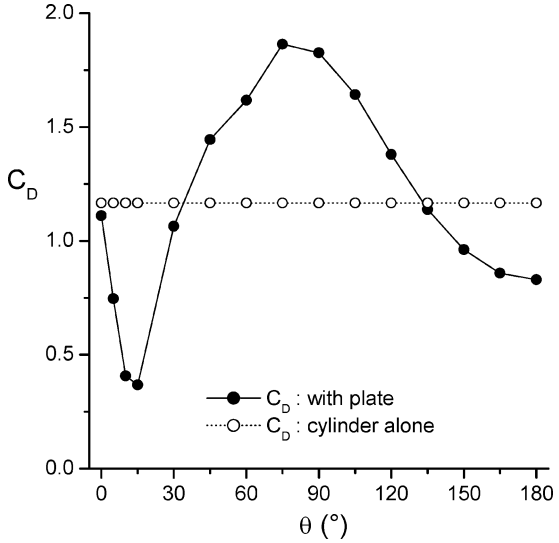

Fig. 10 Drag coefficients on the circular cylinder vs θ.

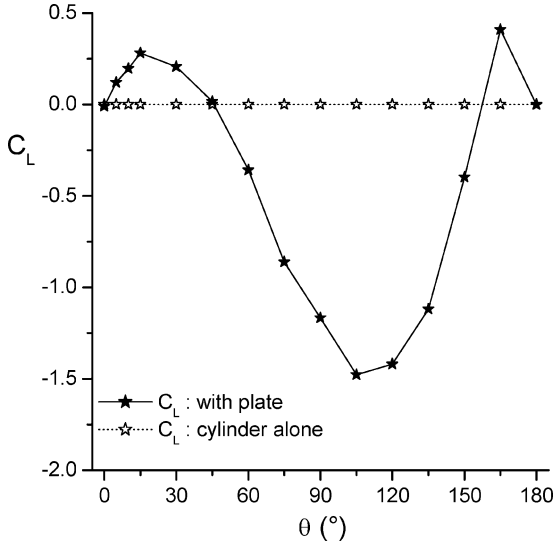

Fig. 11 Lift coefficients on the circular cylinder vs θ.

the drag coefficient is always higher than that of circular cylinder alone.

Similar characteristics can be seen in the variation of the lift coefficient given in Fig. 11. With θ increasing from 0 deg, the symmetry in pressure between lower and upper sides of the circular cylinder breaks and thus the lift coefficient changes. The lift coefficient has two maximum values at the plate angles, $\theta = 15$ and 165 deg, and a minimum value at about $\theta = 105$ deg. It has zero values at about $\theta = 0$, 45, 158, and 180 deg. In fact, at $\theta < 15$ deg, because pressures at $\alpha > \theta$ on the front upper surface of the cylinder are smaller than those at lower region, lift increases upward. From $\theta = 30$ deg, the pressure balance reverses and, thus, the lift coefficient begins to decrease. At $\theta = 45$ deg, pressure distributions in the lower and upper regions of the cylinder are not symmetric. In spite of this, the value of C_L is zero because the pressures balance each other. With further increase in θ, C_L decreases and reaches a minimum value at $\theta = 105$ deg, because at $\theta = 105$ deg the difference between the pressures in the region of $\alpha < 105$ deg and those in the region of $\alpha > 255$ deg is a maximum. At $\theta > 105$ deg, as a result of decrease in pressure level on the front upper surface of the cylinder, C_L begins to increase and reaches a maximum at $\theta = 165$ deg. At $\theta = 180$ deg, because of the symmetry formed as a result of the balancing of the pressures in the lower and upper sides of the cylinder, C_L reaches the beginning value again.

IV. Conclusions

The flow around a circular cylinder with a plate attached to it has been investigated experimentally in the Reynolds number range of 8.0×10^3–6×10^4. In different angles of θ, the influences of the plate on the pressures measured on the surface of circular cylinder, drag and lift coefficients, and vortex-shedding phenomenon are examined and the following results are obtained:

1) In different plate angles, five different types of pressure distributions were observed. The first ones are the well-known pressure distributions measured on the surface of the circular cylinder at $\theta = 0$ and 180 deg and for no plate. The second ones are those measured at smaller plate angles, that is, $\theta = 5$, 10, and 15 deg, where the stagnation point moves to the front lower side of the cylinder. The third ones are the pressure distributions measured at 30 deg $\leq \theta \leq 90$ deg, where the plate influences like a bluff body and the stagnation point occurs on the front upper surface of the cylinder. The fourth type of pressure distribution is measured at 105 deg $\leq \theta \leq 150$ deg. In these pressure distributions separation on the upper side of the cylinder begins again. Another type of pressure distribution is observed at $\theta = 165$ deg, where it has the pressure characteristics of the equilibrium angle.

2) At values of the plate angle of 6 and 162 deg, the Strouhal number has two maximums, whereas it remains almost constant at $\theta = 45$–120 deg. The value of the Strouhal number at $\theta = 180$ deg is 22% smaller than that of the circular cylinder without a plate.

3) Over the Reynolds number range 8×10^3–6.0×10^4, Strouhal numbers were found to be independent of the Reynolds number and the flow type changed only with the plate angle.

4) Drag force on the circular cylinder has a maximum value at approximately $\theta = 75$ deg, whereas it has its minimum value at $\theta = 15$ deg. In the case where the plate behaves as a splitter plate on the back of the cylinder, the drag coefficient is smaller than that of the cylinder alone. Depending on the plate position, the lift force has two maximums, at $\theta = 15$ and 165 deg, whereas it has a zero value at about $\theta = 0$, 45, 158, and 180 deg, where there is no lift.

References

[1]Cimbala, J. M., and Chen, K. T., "Supercritical Reynolds Number Experiments on a Freely Rotatable Cylinder/Splitter Plate Body," *Physics of Fluids*, Vol. 6, No. 7, 1994, pp. 2440–2445.

[2]Anderson, E. A., and Szewczyk, A. A., "Effects of a Splitter Plate on the Near Wake of a Circular Cylinder in 2 and 3-Dimensional Flow Configurations," *Experiments in Fluids*, Vol. 23, 1997, pp. 161–174.

[3]Ozono, S., "Vortex Suppression of the Cylinder Wake by Deflectors," *Journal of Wind Engineering and Industrial Aerodynamics*, Vol. 91, 2003, pp. 91–99.

[4]Mansingh, V., and Oosthuizen, P. H., "Effects of Splitter Plates on the Wake Flow Behind a Bluff Body," *AIAA Journal*, Vol. 28, No. 5, 1990, pp. 778–783.

[5]Nakamura, Y., "Vortex Shedding from Bluff Bodies with Splitter Plates," *Journal of Fluids and Structures*, Vol. 10, 1996, pp. 147–158.

[6]Shiraishi, N., Matsumoto, M., and Shirato, H., "On Aerodynamic Instabilities of Tandem Structures," *Journal of Wind Engineering and Industrial Aerodynamics*, Vol. 23, 1986, pp. 437–447.

[7]Inoaka, K., Yamamoto, J., and Suzuki, K., "Dissimilarity Between Heat Transfer and Momentum Transfer in a Disturbed Turbulent Boundary Layer with Insertion of a Rod—Modeling and Numerical Simulation," *International Journal of Heat and Fluid Flow*, Vol. 20, 1999, pp. 290–301.

[8]Texier, A., Bustamante, A. S. C., and David, L., "Contribution of a Short Separating Plate on the Control of the Swirling Process Downstream a Half-Cylinder," *Experimental Thermal and Fluid Science*, Vol. 26, 2002, pp. 565–572.

[9]Miau, J. J., Yang, C. C., and Chou, J. H., "Suppression of Low-Frequency Variations in Vortex Shedding by a Splitter Plate Behind a Bluff Body," *Journal of Fluids and Structures*, Vol. 7, 1993, pp. 897–912.

[10]Nakagawa, T., "Effects of a Small Airfoil-Shaped Splitter Plate on Vortex Shedding from a Square Prism at Subsonic Mach Numbers," *Acta Mecanica*, Vol. 91, 1992, pp. 11–25.

[11]Xu, J. C., Sen, M., and Gad-El-Hak, M., "Dynamics of a Rotatable Cylinder with Splitter Plate in Uniform Flow," *Journal of Fluids and Structures*, Vol. 7, 1993, pp. 401–416.

[12]Cimbala, J. M., and Garg, S., "Flow in the Wake of a Freely Rotatable Cylinder with Splitter Plate," *AIAA Journal*, Vol. 29, No. 6, 1991, pp. 1001–1003.

[13]Xu, J. C., Sen, M., and Gad-El-Hak, M., "Low-Reynolds Number Flow over a Rotatable Cylinder-Splitter Plate Body," *Physics of Fluids A*, Vol. 2, No. 11, 1990, pp. 1925–1927.

[14]Cimbala, J. M., and Leon, J., "Drag of Freely Rotatable Cylinder/Splitter-Plate Body at Subcritical Reynolds Number," *AIAA Journal,* Vol. 34, No. 11, 1996, pp. 2446–2448.

[15]Rathakrishnan, E., "Effect of Splitter Plate on Bluff Body Drag," *AIAA Journal,* Vol. 37, No. 9, 1999, pp. 1125–1126.

[16]Kwon, S. H., Cho, J. W., Park, J. S., and Choi, H. S., "The Effects of Drag Reduction by Ribbons Attached to Cylindrical Pipes," *Ocean Engineering*, Vol. 29, 2002, pp. 1945–1958.

[17]Sarioglu, M., and Yavuz, T., "Subcritical Flow Around Bluff Bodies," *AIAA Journal*, Vol. 40, No. 7, 2002, pp. 1257–1268.

[18]Roshko, A., "Experiments on the Flow past a Circular Cylinder at Very High Reynolds Number," *Journal of Fluid Mechanics*, Vol. 10, 1961, pp. 345–354.

[19]Apelt, C. J., and West, G. S., "The Effects of Wake Splitter Plates on Bluff Body Flow in the Range $10^4 < \mathrm{Re} < 5 \times 10^4$. Part 2," *Journal of Fluid Mechanics*, Vol. 71, 1975, pp. 145–160.

[20]Ozono, S., "Flow Control of Vortex Shedding by a Short Splitter Plate Asymmetrically Arranged Downstream of a Cylinder," *Physics of Fluids*, Vol. 11, No. 10, 1999, pp. 2928–2934.

[21]Nakamura, Y., "Vortex Shedding from Bluff Bodies and a Universal Strouhal Number," *Journal of Fluids and Structures*, Vol. 10, 1996, pp. 159–171.

[22]Gerrard, J. H., "The Mechanics of the Formation Region of Vortices Behind Bluff Bodies," *Journal of Fluid Mechanics*, Vol. 25, 1966, pp. 401–413.

J. Gore
Associate Editor